Title: Coiled coil control of diverse EGFR functions

Authors: Deepto Mozumdar[1,2], Kim Quach[1], Amy Doerner[1], & Alanna Schepartz[1,2,3,4*]

Affiliations:

[1]Department of Chemistry, Yale University, New Haven, CT 06511

[2]Department of Chemistry, University of California, Berkeley, CA 94705

[3]Department of Molecular and Cell Biology, University of California, Berkeley, CA 94705

[4]California Institute for Quantitative Biosciences, University of California, Berkeley, CA 94720 USA.

*Correspondence: Alanna Schepartz (schepartz@berkeley.edu)

Abstract:

EGFR exhibits biased signaling, whereby growth factor or mutation-dependent changes in receptor conformation and/or dynamics elicit distinct intracellular outcomes. We report that many intracellular EGFR outcomes are controlled by a two-state coiled coil switch located within the juxtamembrane segment (JM), an essential component of the cytosolic dimer interface. The position of this switch defines the path of endocytic trafficking, the extent and dynamics of autophosphorylation, c-Cbl recruitment, and ubiquitination, and whether or not EGFR is degraded within lysosomes. It also predicts kinase-independent effects of oncogenic mutations and clinically relevant tyrosine kinase inhibitors (TKIs) that promote lysosome-based degradation. These findings provide a model for biased EGFR signaling, insights into kinase-independent activities of EGFR and clinically relevant TKIs, and identify new strategies for modulating protein lifetime.

Main text

Receptor tyrosine kinases in the epidermal growth factor receptor family play essential roles in cell proliferation differentiation, and migration (*1*, *2*). Aberrant activation of EGFR family members, whether by overexpression or mutation, is associated with many human cancers (*3*). Although much work on EGFR has focused on its activation by epidermal growth factor (EGF), EGFR is activated by multiple growth factors including transforming growth factor α (TGF-α), epigen, epiregulin,

betacellulin, heparin-binding EGF, and amphiregulin, and transmits these activation events into distinct intracellular phenotypes (*4*–*6*). For decades, growth factor-dependent biased signaling through EGFR has been attributed to differences in the physical properties of the growth factors themselves (*4*, *6*–*8*) or their receptor complexes (*5*, *6*, *8*). EGFR is also activated constitutively by mutations in the kinase domain, the extracellular domain, or elsewhere (*3*); these mutations are causally linked to many human cancers. Here we report that a simple two-state coiled coil switch is necessary and sufficient to define growth factor- and mutation-dependent biased signaling through EGFR.

Previous work has shown that EGFR activation is accompanied by formation of receptor dimers containing one of two isomeric coiled coils within the cytoplasmic juxtamembrane segment (JM) that physically connects the ECD and TM segments to the kinase domain (*9*–*12*). One coiled coil (EGF-type) is characterized by a hydrophobic, leucine-rich interface (*9*, *11*) while the other (TGF-a-type) contains a charged and polar interface (*12*)**.** These coiled coils are rotational isomers that interconvert by virtue of 150 degree disrotatory motion about the helix axis**.** Coiled coil preference is influenced not only by the identity of the activating growth factor (*12*) but also by point mutations within the transmembrane (TM) helix (*13*), oncogenic ECD (*14*) and kinase domain mutations (*15*), and, in the case of drug-resistant L834R/T766M EGFR, kinase domain pharmacologic status (*15*). While it is clear that the JM couples allosterically to the ECD, TM, and kinase domains, this very coupling complicates strategies to define how and whether JM conformational isomerism influences outcomes associated with biased signaling.

To better understand the role of JM conformational isomerism in biased signaling, we designed a set of functional, full-length EGFR variants whose activated dimers favor one JM coiled coil over the other in a manner that is independent of both growth factor identity and kinase domain mutational status (*11*–*14*). This design built on the knowledge that salt bridges at the *e* and *g* positions of

model coiled coils influence stability and orientation (*16*) but not oligomeric state (*17*). Thus we hypothesized that removing salt bridges at the *e* and *g* positions of one JM coiled coil would raise its free energy relative to the other and shift the equilibrium between the two (Fig. S1a). To test this hypothesis, we designed EGFR variants E661R and KRAA (Fig. 1a; Fig. S1b). The single charge-reversing mutation in E661R EGFR eliminates a TGF-α-type-specific salt-bridge, whereas the two charge-eliminating substitutions in K652A/R656A EGFR (KRAA) abolish two EGF-type-specific salt bridges (Fig. 1a). E661R and KRAA EGFR were expressed in CHO-K1 cells and underwent expected auto-phosphorylation within the C-terminal tail when treated with EGF or TGF-α (Fig. S1c). Bipartite tetracysteine display (*11*) confirmed the hypothesis that activated E661R EGFR dimers contained only an EGF-type coiled coil whereas activated KRAA EGFR dimers contained only a TGF-α-type coiled coil (Fig. 1b, Fig. S2). (Fig. 1a).

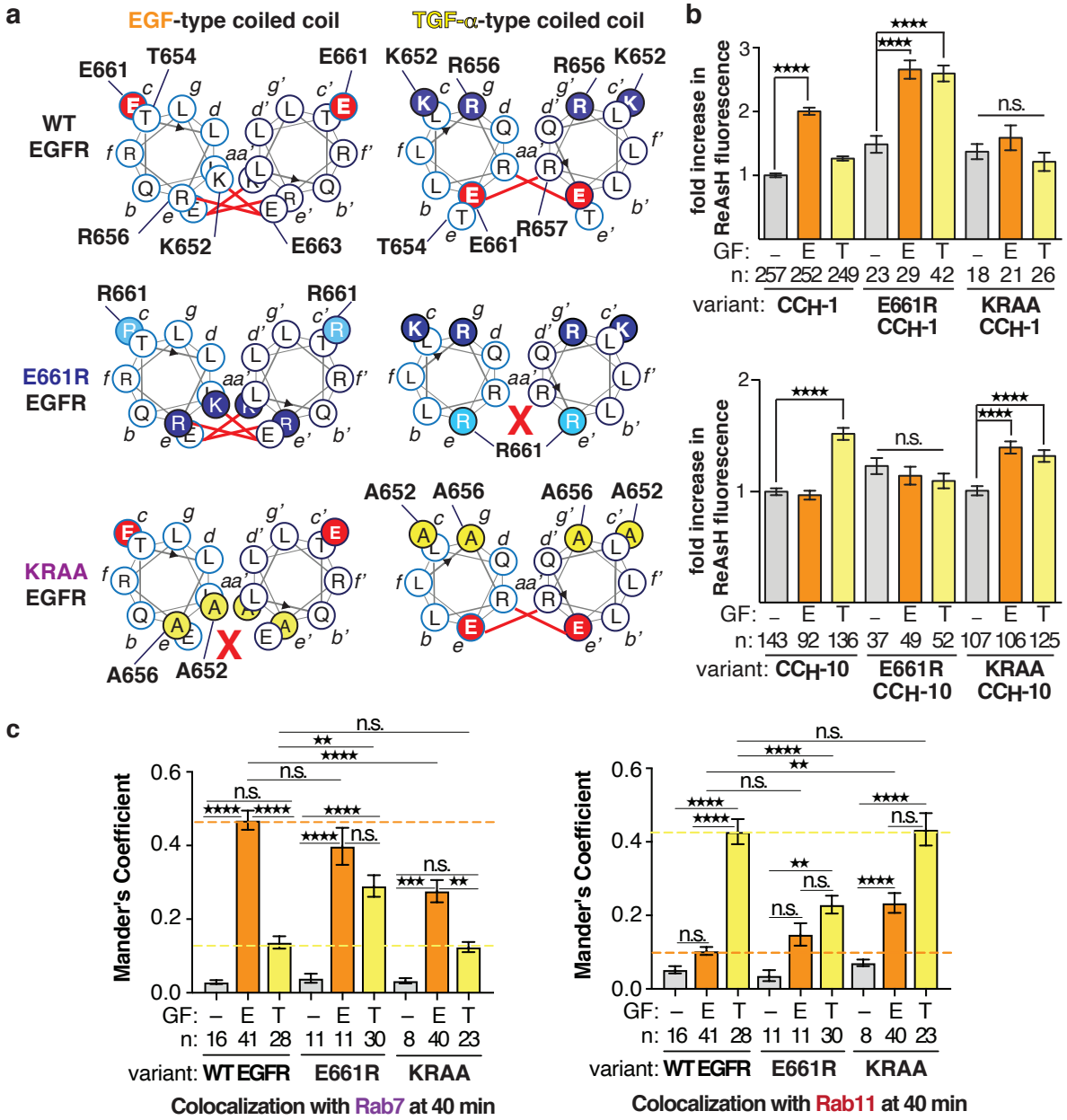

Fig 1: Design of EGFR decoupling mutants. a, Helical wheels illustrating the N-terminal JM segments of WT, E661R, and KRAA EGFR assembled into different coiled coils. b, Expression-corrected ReAsH fluorescence over background. n = # of cells. Error bars = s.e.m. ****p<0.0001, with Dunnett's post-analysis. n.s., not significant. c, Colocalization (MCC) of FLAG-tagged WT, E661R and KRAA EGFR with Rab7 or Rab11-GFP 40 minutes after stimulation without/with EGF/TGF-α. Orange and yellow dashed lines indicate MCC values observed when WT EGFR is stimulated with EGF or TGF-α, respectively. n = # of cells. Error bars = s.e.m. ****p<0.0001, ***p<0.001, **p<0.01, n.s. p>0.05 from one-way ANOVA with Tukey's multiple comparison test.

A quintessential growth factor-dependent EGFR activity is the path of receptor trafficking following endocytosis (*18*, *19*). Activated receptors are trafficked first to EEA1-positive (EEA1+) early endosomes (*19*) and then sorted into vesicles defined by the presence of either Rab11 (Rab11+) or Rab7 (Rab7+). The former recycle EGFR back to the cell surface (*19*) whereas the latter deliver EGFR to late endolysosomes for degradation (*19*). Receptor trafficking is growth factor-dependent: when stimulated with EGF, EGFR traffics into Rab7+ endosomes and is degraded (*20*, *21*); when stimulated with TGF-α, EGFR traffics into Rab11+ endosomes and returns to the cell surface (*20*, *21*). For more than twenty years, the dependence of EGFR trafficking on growth factor identity has been attributed to differences in the pH-dependent ligand occupancy of endocytosed receptors (*4*). Although this model is simple and elegant, it is inconsistent with recent reports that TGF-α-bound EGFR continues to signal within endosomes (*21*). Given the crucial role played by the JM (*9*, *10*, *12*) to connect the sensory (ECD) and effector regions (kinase and C-terminal tail) of the receptor, we sought to explore whether the JM coiled coil itself could influence the path of EGFR trafficking.

We used confocal microscopy to track the time- and growth factor-dependent pattern of EGFR trafficking and colocalization in HeLa cells following growth factor stimulation. As expected, after 8 minutes, all EGFR variants colocalize with early (EEA1+) and not late (Rab7+) or recycling (Rab11+) endosomes (Fig. S3a-d), regardless of whether the cells were stimulated with EGF or TGF-α, and colocalization of all activated receptors with EEA1+ early endosomes decreases after 40 minutes (*20*) (Fig. S4a, b). By contrast, while the extent of colocalization of WT EGFR and T654D EGFR with Rab7 and Rab11 after 40 minutes was growth factor-dependent as expected (Fig. 1c; Fig. S4c, d), the extent of colocalization of E661R and KRAA EGFR with Rab7 and Rab11 depended on both growth factor identity and coiled coil status: E661R EGFR colocalized significantly with Rab7, and KRAA EGFR colocalized significantly with Rab11, regardless of whether the receptor was activated with EGF or TGF-α (Fig. 1c.). These results indicate that JM coiled coil status alone can bias the path of EGFR trafficking. We note, however, that the bias is incomplete: while E661R EGFR favors a path into Rab7+ endosomes, and KRAA EGFR favors a path into

Rab11+ endosomes, a small fraction of TGF-α-activated E661R-EGFR traffics into Rab11+ endosomes, and a small fraction of EGF-activated KRAA EGFR traffics into Rab7+ endosomes.

Mindful of the fact that both E661R and KRAA EGFR contain mutations within the JM coiled coil itself, we turned to a set of EGFR variants in which JM coiled coil identity is controlled by point mutations in the adjacent TM segment (*13*). Substitution of phenylalanine for a single glycine (G628) at the final position of the N-terminal G-x-x-G motif of the EGFR TM (G628F EGFR) generates a receptor dimer with an EGF-type JM coiled coil, regardless of whether the receptor is activated by either EGF or TGF-α–just like E661R EGFR. Likewise, substitution of valine at position 628 (G628V EGFR) generates a receptor dimer with a TGF-α-type coiled coil, regardless of whether the receptor is activated by either EGF or TGF-α–just like KRAA EGFR (*13*). Since these TM variants contain a wild-type JM, the trafficking patterns they follow provide an unadulterated view of the relationship between JM conformational status and EGFR trafficking. If JM coiled coil structure is both necessary and sufficient to direct the pathway of EGFR trafficking, then G628F and G628V EGFR should traffic into only Rab7+ or Rab11+ endosomes, respectively, regardless of how they are activated, whereas G628A EGFR should behave like WT EGFR and traffic in a growth factor-dependent manner. Control experiments verified that G628F, G628V, and G628A EGFR colocalize initially with EEA1 (Fig. S5a, d) and not with Rab7 or Rab11 (Fig. S5b, e); colocalization with EEA1 falls to expected levels after 40 min (Fig. S5c, f).

Indeed, after 40 minutes, although the extent of G628A EGFR colocalization with Rab7 and Rab11 was growth factor-dependent, the colocalization of G628F and G628V EGFR were not (Fig. 2a, b). When stimulated with EGF, G628A EGFR colocalized preferentially with Rab7 and not Rab11; when stimulated with TGF-α, G628A EGFR colocalized preferentially with Rab11 and not Rab7. By contrast, G628F EGFR colocalizes exclusively with Rab7 whether stimulated with EGF or TGF-α and not with Rab11. Conversely, G628V EGFR colocalizes exclusively with Rab11 whether

stimulated with EGF or TGF-α and not with Rab7. Here, when JM coiled coil status is controlled allosterically by distal mutations, the switch in trafficking pattern was complete: G628F EGFR, whose JM contains an EGF-type coiled coil, traffics along the degradative pathway whereas G628V EGFR, whose JM contains a TGF-type coiled coil, traffics along the recycling pathway.

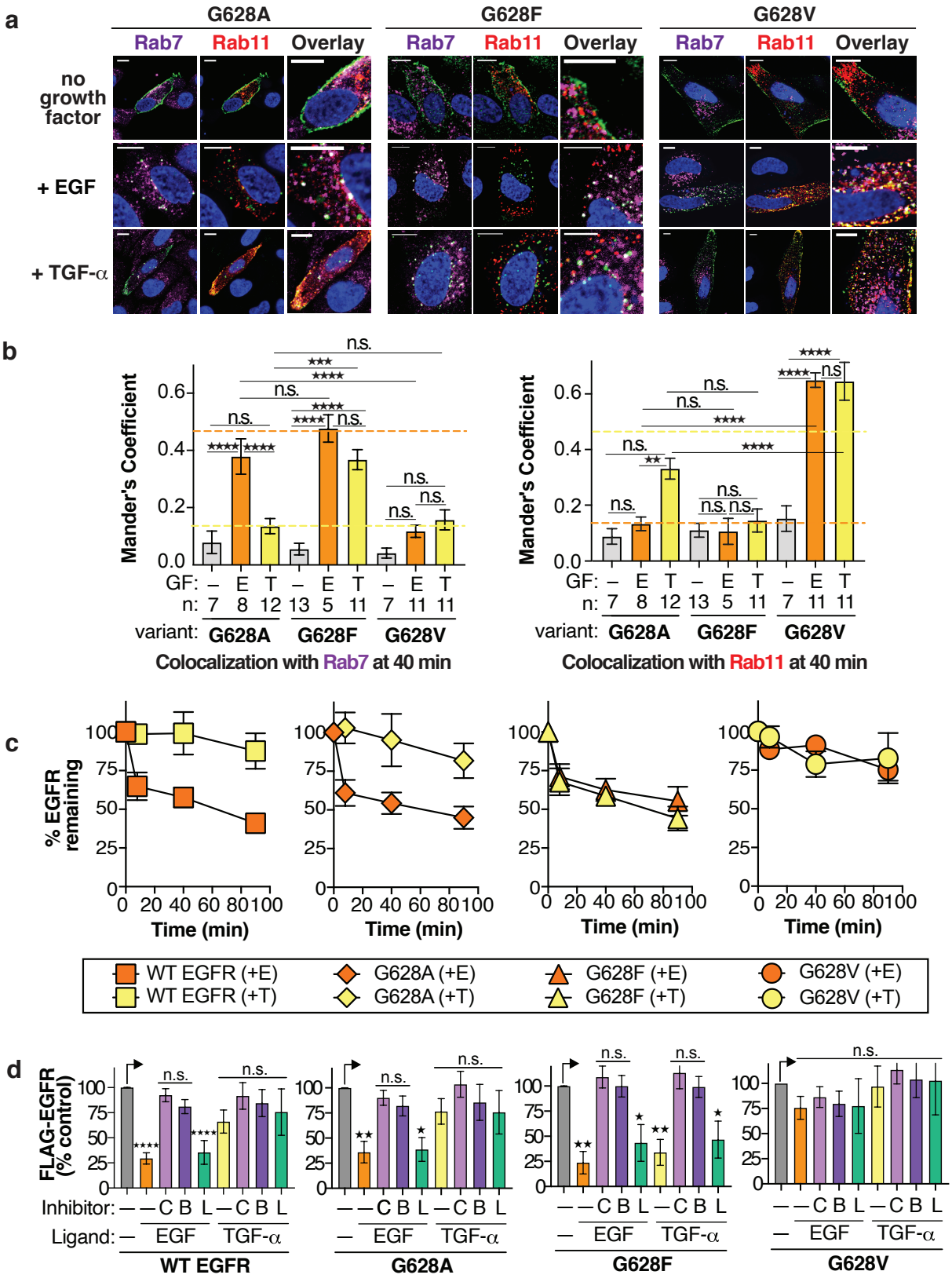
a
G628A
G628F
G628V
Rab7
Rab11
Overlay
no growth factor
+ EGF
+ TGF-α
b
Mander's Coefficient
GF: – E T – E T – E T
n: 7 8 12 13 5 11 7 11 11
variant: G628A G628F G628V
Colocalization with Rab7 at 40 min
Colocalization with Rab11 at 40 min
c
% EGFR remaining
Time (min)
WT EGFR (+E)
WT EGFR (+T)
G628A (+E)
G628A (+T)
G628F (+E)
G628F (+T)
G628V (+E)
G628V (+T)
d
FLAG-EGFR (% control)
Inhibitor: — — C B L — C B L
Ligand: — EGF TGF-α
WT EGFR
G628A
G628F
G628V

Fig. 2: Point mutations within the EGFR TM allosterically influence receptor trafficking. a, Confocal microscopy of HeLa cells expressing G628A, G628F and G628V EGFR (green) and Rab11-GFP (red), 40 minutes after stimulation without/ with EGF/TGF-α. Degradative endosomes (purple) are identified using anti-Rab7 antibody. Scale bars = 10 μm. b, Co-localization of FLAG-tagged G628A, G628F and G628V EGFR with Rab7/Rab11-GFP 40 minutes after stimulation with EGF/TGF-α. n = # of cells. Error bars = s.e.m. Orange/yellow dashed lines indicate co-localization of WT EGFR with endocytic marker when stimulated with EGF/TGF-α respectively. s.e.m. ****$p<0.0001$, ***$p<0.001$, **$p<0.01$, n.s. $p>0.05$ from one-way ANOVA with Tukey's multiple comparison test. c, Normalized % intact EGFR detected 0-90 minutes after stimulation with EGF/TGF-α. d, Quantified % intact EGFR detected in HeLa cells 90 minutes after stimulation without/with EGF/TGF-α and/or 100 μM chloroquine ©, 250 nM bafilomyin (B) or 10 μM Lactacystin (L) for 1 hour at 37°C. Error bars = s.e.m. ****$p<0.0001$, **$p<0.01$, *$p<0.05$ with Dunnett's post-analysis. n.s., not significant.

These differences in trafficking led to predictable changes in EGFR lifetime (Fig. 2c; Fig. S6a). The lifetime of WT and G628A EGFR depends on growth factor identity in the expected way (*8*, *20*, *21*). Following EGF stimulation, WT and G628A EGFR levels decrease rapidly and the fraction of intact receptor detected after 90 minutes is low (41-45%), whereas the levels of both receptors remain steady when cells are stimulated with TGF-α, and the fraction of intact EGFR detected after 90 minutes is high (82-88%). By contrast, G628F EGFR was degraded rapidly regardless of whether the receptor was activated with EGF or TGF-α, with 55% and 44% of the intact receptor remaining after 90 min following EGF or TGF-α treatment, respectively. Conversely, G628V was degraded slowly, with 75% and 83% of the intact receptor remaining following EGF and TGF-α treatment, respectively. Thus, the presence of a single point mutation in the TM segment and its long-range effect on JM conformation are necessary and sufficient to dictate the pathway of intracellular trafficking and extent of EGFR degradation. Control experiments confirmed that EGFR degradation occurred within lysosomes (Fig. 2d; Fig. S6b). These results support a model in which the path of endocytic trafficking following EGFR activation is determined by JM coiled coil status and not simply by growth factor-dependent differences in the EGFR-ligand complex stability as previously proposed (*4*, *20*, *21*). The different effects of EGFR-selective growth factors also do not correlate with receptor dimer strength (*6*) as EGF and TGF-α both induce high affinity ECD dimers but traffic differently and induce different MCF-7 cell states (Fig. S7).

Upon activation with EGF, EGFR undergoes c-Cbl mediated (*22*) poly-ubiquitination (*23*), which guides the receptor into degradative endosomes (*24*, *25*). c-Cbl is recruited to EGF-activated EGFR by phosphorylated C-terminal tail residues: Y1045, Y1068, and Y1086 (*26*). The extent and kinetics of Y1045, Y1068 and Y1086 phosphorylation, c-Cbl recruitment, and EGFR poly-ubiquitination correlate with growth factor identity (*20*). Following EGF activation, these signals are elevated and sustained (*20*, *8*); with TGF-α activation, the signals are low and transient (*20*, *8*). The transient TGF-α-induced signals have also been attributed to the rapid dissociation of TGF-α from EGFR in early endosomes (*4*). Given that JM coiled coil status controls EGFR trafficking and lifetime (Fig. 1-2), we hypothesized that it would also bias the growth factor-dependent patterns of C-terminal tail phosphorylation (at Y1045/ Y1068), c-Cbl recruitment, and receptor poly-ubiquitination.

To test this hypothesis, HeLa cells expressing WT, G628A, G628F, or G628V EGFR were treated with EGF or TGF-α and immunoblots were used to follow the time-dependent phosphorylation at Y1045 or Y1068 (Fig. 3a-d) and Y1173 (Fig. S6c,d), which is not involved in c-Cbl recruitment (*26*). With WT and G628A EGFR, stimulation with EGF led to higher pY1045 and pY1068 levels than with TGF-α, where the signal decays rapidly (Fig. 5a-d), as expected from previous reports (*8*, *20*). With G628F EGFR, the pattern of phosphorylation mirrored that of EGF-stimulated WT/ G628A EGFR, regardless of whether the cells were stimulated with EGF or TGF-α. With G628V EGFR, the pattern of phosphorylation mirrored TGF-α-stimulated WT/ G628A EGFR, regardless of whether the cells were stimulated with EGF or TGF-α. The time-dependent patterns of c-Cbl recruitment are also coiled coil dependent (Fig. 3e, f). Although all growth factor-activated EGFR variants are modified primarily K63- and not K48-linked polyubiquitin chains (*24*, *25*), the extent of polyubiquitination was higher for EGF-stimulated WT/ G628A EGFR and for G628F regardless of growth factor identity, and lower for G628V EGFR (Fig. S6e). Overall, the pattern of C-terminal tail phosphorylation (at Y1045, Y1068 and Y1173) c-Cbl recruitment, and extent of K63-linked polyubiquitination are all dictated by the structure of EGFR within the JM (Fig. S6f) and not simply by pH-dependent differences in receptor occupancy or lifetime.

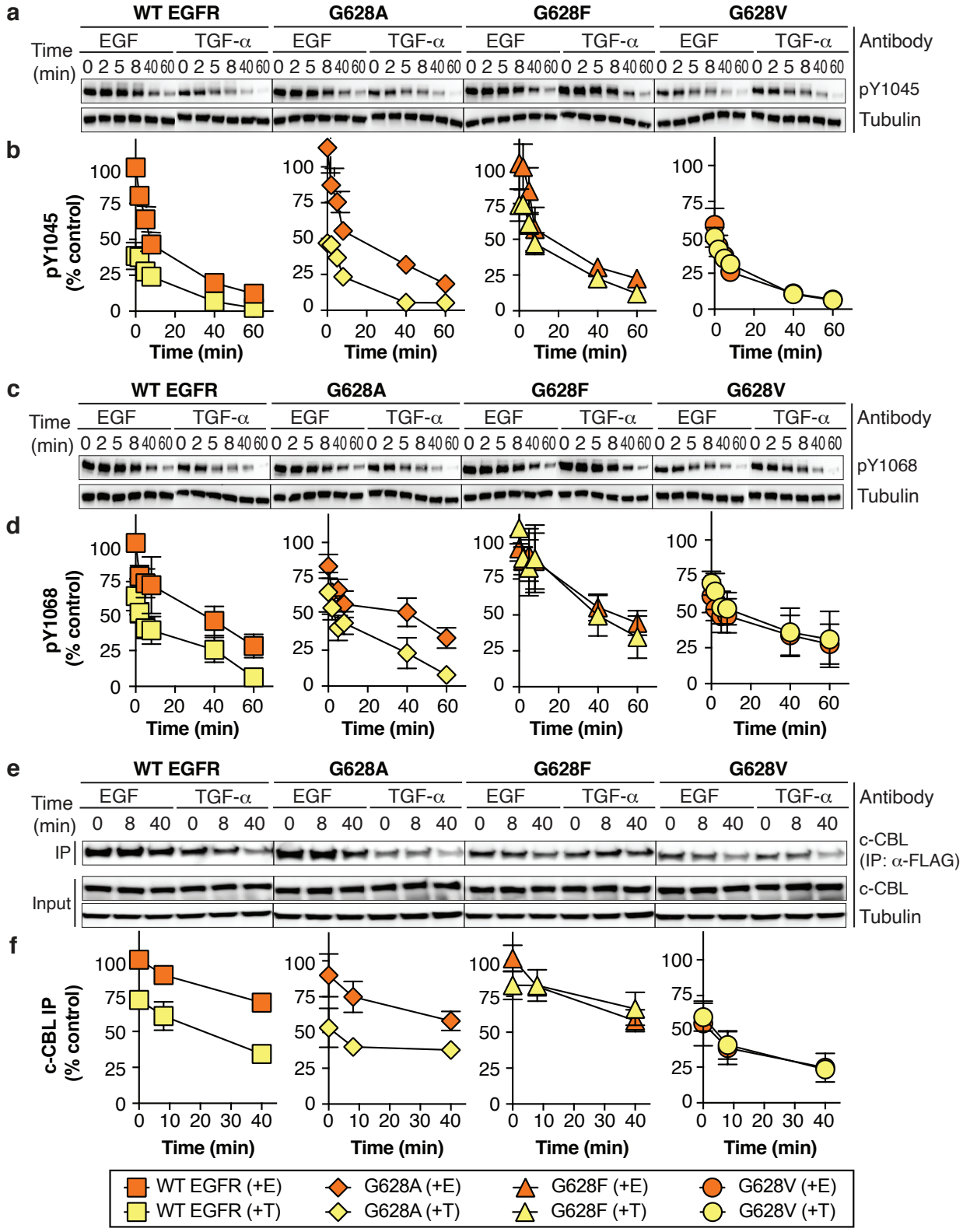

Fig 3: The EGFR JM controls C-terminal tail autophosphorylation kinetics and c-Cbl recruitment

status. Time-dependent change in a, pY1045; c, pY1068; and e, c-Cbl recruitment 0-60 minutes after stimulation with EGF or TGF-α (16.7 nM). b, d, f, Plots quantifying changes in Fig 3. a, c, e.

The allosteric network coordinating information transfer between the ECD, TM, and JM regions of EGFR also includes the kinase domain and its pharmacologic state (*13*, *15*, *27*). Kinase domain mutations associated with drug-resistant non-small cell lung cancer (L834R/T766M) (*28*) generate constitutively active receptors whose JM favors a TGF-α-type structure (*15*). The JM coiled coil shifts into the EGF-type structure when L834R/T766M EGFR is inhibited by third-generation TKIs such as WZ-4002, CO-1686, or the clinically approved AZD-9291 (*29*, *30*). Using confocal microscopy, we evaluated the pattern of endocytic trafficking and sub-cellular localization of L834R/T766M EGFR in HeLa cells in the presence and absence of second- (afatinib), third- (AZD-9291), and fourth-generation (EAI045) TKIs (*29*, *30*) that differ in mechanism of engagement (covalent vs. non-covalent), EGFR specificity (WT vs. DM; monomer vs. dimer-specific), and binding site (ATP vs. allosteric) (Fig. 4). All inhibitors decreased the levels of EGFR auto-phosphorylation (Fig. S8a). We observed that after 40 min uninhibited and afatinib-inhibited L834R/T766M EGFR colocalize with Rab11 and not Rab7 (Fig. 4a, b), favoring the recycling pathway expected for activated receptors that contain a TGF-α-type JM coiled coil (*15*). By contrast, when covalently inhibited by AZD-9291, the colocalization of L834R/T766M EGFR with Rab7 increases and colocalization with Rab11 decreases. Similar changes in the receptor trafficking pathway were observed when cells expressing L834R/T766M EGFR were treated with the fourth-generation inhibitor EAI045, which binds noncovalently in a pocket adjacent to that of AZD9291 (*30*). AZD-9291 and EAI045 differ in both engagement mode and binding site within the EGFR kinase domain, suggesting that the change in receptor trafficking results from allosteric changes in EGFR structure and not recognition of a composite small molecule-protein surface (*31*)

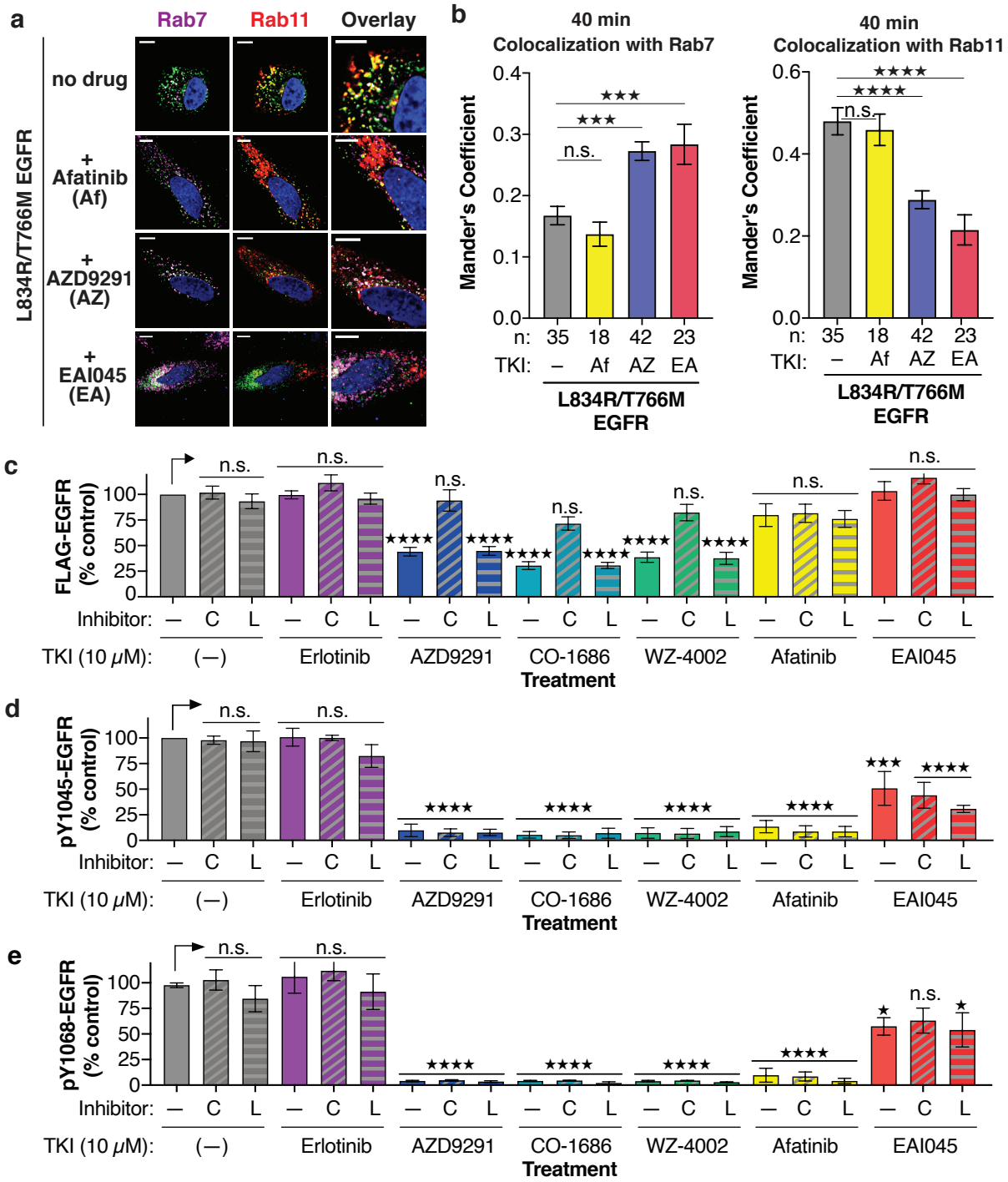

Fig 4: TKIs influence the trafficking and lifetime of oncogenic L834R/T766M EGFR a, Confocal microscopy of HeLa cells expressing FLAG-tagged L834R/T766M EGFR (green) and Rab11-GFP (red) as a marker for recycling endosomes, 30 minutes after pre-incubation without/with 10 μM of afatinib (Af), AZD-9291 (AZ) or EAI045 (EA). Degradative endosomes (purple) identified using an anti-Rab7 antibody. Scale bars = 10 μm. b, Co-localization of FLAG-tagged L834R/T766M EGFR with Rab7 or Rab11 without/with the indicated TKI. n = # of cells. Error bars = s.e.m. ****p<0.0001, ***p<0.001, **p<0.01, *p<0.05, n.s. p>0.05 from one-way ANOVA with Dunnett's multiple

comparison. c, Normalized loss of FLAG-tagged L834R/T766M EGFR in HeLa cells 12 hours following pre-incubation without/with 100 μM chloroquine (C) or lactacystin (L) (10 μM) and/or 10 μM Erlotinib (Er), afatinib (Af), AZD9291 (AZ), CO-1686 (CO), WZ-4002 (WZ), or EAI045 (EA). Phosphorylation of L834R/T766M EGFR at d, Y1045; and e, Y1068 in HeLa cell lysates prepared as described in 7C. In B,D,F, Error bars = s.e.m. ****$p<0.0001$, ***$p<0.001$, n.s. $p>0.05$ from one-way ANOVA with Dunnett's multiple comparison test.

We also evaluated the extent of L834R/T766M EGFR degradation in the presence of second-, third- and fourth-generation inhibitors to determine if JM coiled coil status also uniquely determined EGFR lifetime. Both uninhibited and afatinib-treated L834R/T766M EGFR levels remained steady at early (8, 40, 90 min) (Fig. S8b) and late (12 hours) (Fig. 4c; Fig. S8c) time points. In contrast, treatment of L834R/T766M EGFR with AZD-9291 led to markedly (> 50%) reduced receptor levels of after 12 hours when compared to untreated samples (Fig. 4c; Fig. S8C). Similar reductions were observed 12 hours after treatment with two other third-generation TKIs, WZ-4002 and CO-1686 but not EAI1045 (Fig. 4c; Fig. S8c). Thus, in all cases examined, covalent, third-generation TKIs that engage the ATP-binding pocket (*29*, *30*), allosterically induce an EGF-type structure within the JM (*15*), and traffic the receptor into Rab7+ endolysosomes (this work), also induce L834R/T766M EGFR degradation. The TKI-induced degradation of L834R/T766M EGFR is entirely lysosomal. Little or no ubiquitination of L834R/T766M EGFR is observed in the presence of any TKI (Fig. S8f). These results suggest that TKI-dependent sorting of L834R/T766M EGFR into alternative arms of the endocytic pathway and its effect on receptor lifetime may be an unrecognized kinase-independent function of oncogenic EGFR mutations and their inhibition by clinically relevant third-generation TKIs. It also implies that AZD-9291-inhibited L834R/T766M EGFR is recognized by one or more as-yet unidentified factors that deliver the receptor into degradative cellular compartments and could be co-opted as a novel form of lysosome-based protein degradation.

References and Notes.

Acknowledgements. Funding: This work was supported by the NIH (RO1 GM83257 and R35

GM134963 to A.S.). D.M. and A.D. acknowledge support provided by an NIH Training Grant in Biophysics (5T32GM008283).**Authors contributions:** D.M., K.Q., A.D., and A.S. designed experiments. D.M., K.Q., and A.D. performed experiments. D.M., K.Q., A.D. and A.S. wrote the paper**. Competing interests:** The authors declare no competing interests. **Data and Materials Availability:** All data is available in the manuscript or the supplementary materials.

Supplementary Materials

Materials and Methods

Table S1

Fig S1–8

References (*32*–*34*)

References

1. M. A. Lemmon, J. Schlessinger, Cell signaling by receptor tyrosine kinases. *Cell*. **141**, 1117–34 (2010).

2. E. Kovacs, J. A. Zorn, Y. Huang, T. Barros, J. Kuriyan, A structural perspective on the regulation of the epidermal growth factor receptor. *Annu Rev Biochem*. **84**, 739–64 (2015). 3. S. Sigismund, D. Avanzato, L. Lanzetti, Emerging functions of the EGFR in cancer. *Mol. Oncol.* **12**, 3–20 (2018).

4. A. R. French, D. K. Tadaki, S. K. Niyogi, D. A. Lauffenburger, Intracellular trafficking of epidermal growth factor family ligands is directly influenced by the pH sensitivity of the receptor/ligand interaction. *J Biol Chem*. **270**, 4334–40 (1995).

5. T. Ronan, J. L. Macdonald-Obermann, L. Huelsmann, N. J. Bessman, K. M. Naegle, L. J. Pike, Different Epidermal Growth Factor Receptor (EGFR) Agonists Produce Unique

Signatures for the Recruitment of Downstream Signaling Proteins. *J Biol Chem*. **291**, 5528–40 (2016).

6. D. M. Freed, N. J. Bessman, A. Kiyatkin, E. Salazar-Cavazos, P. O. Byrne, J. O. Moore, C. C. Valley, K. M. Ferguson, D. J. Leahy, D. S. Lidke, M. A. Lemmon, EGFR Ligands Differentially Stabilize Receptor Dimers to Specify Signaling Kinetics. *Cell*. **171**, 683-695 e18 (2017).

7. J. T. Jones, R. W. Akita, M. X. Sliwkowski, Binding specificities and affinities of egf domains for ErbB receptors. *FEBS Lett*. **447**, 227–31 (1999).

8. K. E. Longva, F. D. Blystad, E. Stang, A. M. Larsen, L. E. Johannessen, I. H. Madshus, Ubiquitination and proteasomal activity is required for transport of the EGF receptor to inner membranes of multivesicular bodies. *J Cell Biol*. **156**, 843–54 (2002).

9. N. Jura, N. F. Endres, K. Engel, S. Deindl, R. Das, M. H. Lamers, D. E. Wemmer, X. Zhang, J. Kuriyan, Mechanism for activation of the EGF receptor catalytic domain by the juxtamembrane segment. *Cell*. **137**, 1293–307 (2009).

10. M. R. Brewer, S. H. Choi, D. Alvarado, K. Moravcevic, A. Pozzi, M. A. Lemmon, G. Carpenter, The Juxtamembrane Region of the EGF Receptor Functions as an Activation Domain. *Mol. Cell*. **34**, 641–651 (2009).

11. R. A. Scheck, M. A. Lowder, J. S. Appelbaum, A. Schepartz, Bipartite tetracysteine display reveals allosteric control of ligand-specific EGFR activation. *ACS Chem Biol*. **7**, 1367–76 (2012).

12. A. Doerner, R. Scheck, A. Schepartz, Growth Factor Identity Is Encoded by Discrete Coiled-Coil Rotamers in the EGFR Juxtamembrane Region. *Chem Biol*. **22**, 776–84 (2015).

13. J. K. L. Sinclair, A. S. Walker, A. E. Doerner, A. Schepartz, Mechanism of Allosteric Coupling into and through the Plasma Membrane by EGFR. *Cell Chem Biol*. **25**, 857-870 e7 (2018).

14. D. Mozumdar, A. E. Doerner, J. Zhang, D. Rafizadeh, A. Schepartz, Discrete coiled coil rotamers form within the EGFRvIII juxtamembrane domain. *Biochemistry* (2020), doi:10.1021/acs.biochem.0c00641.

15. M. A. Lowder, A. E. Doerner, A. Schepartz, Structural Differences between Wild-Type and Double Mutant EGFR Modulated by Third-Generation Kinase Inhibitors. *J Am Chem Soc*. **137**,

6456–9 (2015).

16. E. K. O'Shea, K. J. Lumb, P. S. Kim, Peptide "Velcro": design of a heterodimeric coiled coil. *Curr Biol*. **3**, 658–67 (1993).

17. P. B. Harbury, T. Zhang, P. S. Kim, T. Alber, A switch between two-, three-, and four-stranded coiled coils in GCN4 leucine zipper mutants. *Science*. **262**, 1401–7 (1993). 18. P. J. Cullen, F. Steinberg, To degrade or not to degrade: mechanisms and significance of endocytic recycling. *Nat. Rev. Mol. Cell Biol.* **19**, 679–696 (2018).

19. J. Bakker, M. Spits, J. Neefjes, I. Berlin, The EGFR odyssey - from activation to destruction in space and time. *J Cell Sci*. **130**, 4087–4096 (2017).

20. K. Roepstorff, M. V. Grandal, L. Henriksen, S. L. Knudsen, M. Lerdrup, L. Grovdal, B. M. Willumsen, B. van Deurs, Differential effects of EGFR ligands on endocytic sorting of the receptor. *Traffic*. **10**, 1115–27 (2009).

21. C. Francavilla, M. Papetti, K. T. Rigbolt, A. K. Pedersen, J. O. Sigurdsson, G. Cazzamali, G. Karemore, B. Blagoev, J. V. Olsen, Multilayered proteomics reveals molecular switches dictating ligand-dependent EGFR trafficking. *Nat Struct Mol Biol*. **23**, 608–18 (2016).

22. H. Waterman, G. Levkowitz, I. Alroy, Y. Yarden, The RING finger of c-Cbl mediates desensitization of the epidermal growth factor receptor. *J Biol Chem*. **274**, 22151–4 (1999). 23. F. Huang, X. Zeng, W. Kim, M. Balasubramani, A. Fortian, S. P. Gygi, N. A. Yates, A. Sorkin, Lysine 63-linked polyubiquitination is required for EGF receptor degradation. *Proc Natl Acad Sci U A*. **110**, 15722–7 (2013).

24. K. Haglund, I. Dikic, The role of ubiquitylation in receptor endocytosis and endosomal sorting. *J Cell Sci*. **125**, 265–75 (2012).

25. C. Raiborg, H. Stenmark, The ESCRT machinery in endosomal sorting of ubiquitylated membrane proteins. *Nature*. **458**, 445–52 (2009).

26. F. Capuani, A. Conte, E. Argenzio, L. Marchetti, C. Priami, S. Polo, P. P. Di Fiore, S. Sigismund, A. Ciliberto, Quantitative analysis reveals how EGFR activation and downregulation are coupled in normal but not in cancer cells. *Nat. Commun.* **6**, 1–14 (2015).

27. J. L. Macdonald-Obermann, L. J. Pike, Allosteric regulation of epidermal growth factor (EGF) receptor ligand binding by tyrosine kinase inhibitors. *J. Biol. Chem.* **293**, 13401–13414 (2018).

28. T. J. Lynch, R. A. Okimoto, J. G. Supko, J. Settleman, Activating Mutations in the Epidermal Growth Factor Receptor Underlying Responsiveness of Non–Small-Cell Lung Cancer to Gefitinib. *N. Engl. J. Med.*, 11 (2004).

29. F. M. Ferguson, N. S. Gray, Kinase inhibitors: the road ahead. *Nat. Rev. Drug Discov.* **17**, 353–377 (2018).

30. Y. Jia, C.-H. Yun, E. Park, D. Ercan, M. Manuia, J. Juarez, C. Xu, K. Rhee, T. Chen, H. Zhang, S. Palakurthi, J. Jang, G. Lelais, M. DiDonato, B. Bursulaya, P.-Y. Michellys, R. Epple, T. H. Marsilje, M. McNeill, W. Lu, J. Harris, S. Bender, K.-K. Wong, P. A. Jänne, M. J. Eck, Overcoming EGFR(T790M) and EGFR(C797S) resistance with mutant-selective allosteric inhibitors. *Nature*. **534**, 129–132 (2016).

31. C. J. Gerry, S. L. Schreiber, Unifying principles of bifunctional, proximity-inducing small molecules. *Nat. Chem. Biol.* **16**, 369–378 (2020).

32. C. A. Schneider, W. S. Rasband, K. W. Eliceiri, NIH Image to ImageJ: 25 years of Image Analysis. *Nat. Methods*. **9**, 671–675 (2012).

33. K. W. Dunn, M. M. Kamocka, J. H. McDonald, A practical guide to evaluating colocalization in biological microscopy. *Am. J. Physiol. - Cell Physiol.* **300**, C723–C742 (2011). 34. S. Bolte, F. P. Cordelières, A guided tour into subcellular colocalization analysis in light microscopy. *J. Microsc.* **224**, 213–232 (2006).